



Prognostic Impact of Myocardial Extracellular Volume Fraction Assessment Using Dual-Energy Computed Tomography in Patients Treated With Aortic Valve Replacement for Severe Aortic...

Suzuki, Masataka ; Toba, Takayoshi ; Izawa, Yu ; Fujita, Hiroshi ;
Miwa, Keisuke ; Takahashi, Yu ; Toh, Hiroyuki ; Kawamori, Hiroyuki ;...

(Citation)

Journal of the American Heart Association, 10(18):e020655

(Issue Date)

2021-09-21

(Resource Type)

journal article

(Version)

Version of Record

(Rights)

© 2021 The Authors. Published on behalf of the American Heart Association, Inc., by Wiley Blackwell.

This is an open access article under the terms of the Creative Commons Attribution-NonCommercial-NoDerivs License, which permits use and distribution in any medium,...




(URL)

<https://hdl.handle.net/20.500.14094/90008620>



ORIGINAL RESEARCH

Prognostic Impact of Myocardial Extracellular Volume Fraction Assessment Using Dual-Energy Computed Tomography in Patients Treated With Aortic Valve Replacement for Severe Aortic Stenosis

Masataka Suzuki, MD; Takayoshi Toba , MD, PhD; Yu Izawa, MD; Hiroshi Fujita, MD; Keisuke Miwa, MD; Yu Takahashi, MD; Hiroyuki Toh, MD; Hiroyuki Kawamori, MD, PhD; Hiromasa Otake , MD, PhD; Hidekazu Tanaka, MD, PhD; Sei Fujiwara, MD, PhD; Yoshiaki Watanabe, MD, PhD; Atsushi K. Kono , MD, PhD; Kenji Okada, MD, PhD; Ken-ichi Hirata, MD, PhD

BACKGROUND: Myocardial extracellular volume fraction (ECV), measured by cardiac magnetic resonance imaging, is a useful prognostic marker for patients who have undergone aortic valve replacement (AVR) for aortic stenosis. However, the prognostic significance of ECV measurements based on computed tomography (CT) is unclear. This study evaluated the association between ECV measured with dual-energy CT and clinical outcomes in patients with aortic stenosis who underwent transcatheter or surgical AVR.

METHODS AND RESULTS: We retrospectively enrolled 95 consecutive patients (age, 84.0 ± 5.0 years; 75% women) with severe aortic stenosis who underwent preprocedural CT for transcatheter AVR planning. ECV was measured using iodine density images obtained by delayed enhancement dual-energy CT. The primary end point was a composite outcome of all-cause death and hospitalization for heart failure after AVR. The mean ECV measured with CT was $28.1 \pm 3.8\%$. During a median follow-up of 2.6 years, 22 composite outcomes were observed, including 15 all-cause deaths and 11 hospitalizations for heart failure. In Kaplan-Meier analysis, the high ECV group ($\geq 27.8\%$ [median value]) had significantly higher rates of composite outcomes than the low ECV group ($< 27.8\%$) (log-rank test, $P = 0.012$). ECV was the only independent predictor of adverse outcomes on multivariable Cox regression analysis (hazards ratio, 1.25; 95% CI, 1.10–1.41; $P < 0.001$).

CONCLUSIONS: Myocardial ECV measured with dual-energy CT in patients who underwent aortic valve intervention was an independent predictor of adverse outcomes after AVR.

Key Words: aortic stenosis ■ computed tomography ■ extracellular volume fraction

Aortic stenosis (AS) is a progressive disease of the myocardium, as well as the aortic valve itself, which causes continuous pressure overload on the left ventricle, leading to cardiac remodeling, myocardial hypertrophy, and finally myocardial fibrosis,¹ a

key determinant of cardiac dysfunction in patients with severe AS.^{2,3} As the disease progresses, the pathological changes, including fibrotic replacement, become uncontrollable, even by aortic valve replacement (AVR), resulting in further impaired cardiac function and poor

Correspondence to: Takayoshi Toba, MD, PhD, Division of Cardiovascular Medicine, Department of Internal Medicine, Kobe University Graduate School of Medicine, 7-5-1 Kusunoki-cho, Chuo-ku, Kobe, Hyogo, 650-0017, Japan. E-mail: taka02222003@gmail.com

Supplementary Materials for this article is available at <https://www.ahajournals.org/doi/suppl/10.1161/JAHA.120.020655>

For Sources of Funding and Disclosures, see page 11.

© 2021 The Authors. Published on behalf of the American Heart Association, Inc., by Wiley. This is an open access article under the terms of the Creative Commons Attribution-NonCommercial-NoDerivs License, which permits use and distribution in any medium, provided the original work is properly cited, the use is non-commercial and no modifications or adaptations are made.

JAHA is available at: www.ahajournals.org/journal/jaha

CLINICAL PERSPECTIVE

What Is New?

- Myocardial extracellular volume fraction, derived from dual-energy computed tomography, was the independent predictor for composite outcomes of all-cause death and hospitalization for heart failure in patients with severe aortic stenosis who underwent transcatheter or surgical aortic valve replacement.

What Are the Clinical Implications?

- In transcatheter aortic valve replacement candidates, myocardial extracellular volume fraction measurement with dual-energy computed tomography is valuable for predicting prognosis after aortic valve replacement and reasonable because it can be easily measured by adding delayed myocardial enhancement imaging to the routine preprocedural computed tomography imaging.

Nonstandard Abbreviations and Acronyms

AS	aortic stenosis
AVR	aortic valve replacement
E	early diastolic transmitral flow velocity
e'	early diastolic mitral annular velocity
ECV	extracellular volume fraction
SAVR	surgical aortic valve replacement
STS-PROM	Society of Thoracic Surgeons Predicted Risk of Mortality
TAVR	transcatheter aortic valve replacement

prognosis.⁴ Therefore, evaluation of myocardial fibrosis is crucial for considering the appropriate therapeutic strategy and predicting prognosis.

To assess myocardial fibrosis noninvasively, cardiac magnetic resonance (CMR) has been widely implemented. Late gadolinium enhancement is a well-validated technique for visually assessing focal replacement fibrosis, but it has limitations in detecting mild focal fibrosis and underestimates diffuse fibrosis. Myocardial extracellular volume fraction (ECV) measurement, using the T1-mapping technique, has been developed to overcome these limitations, allowing quantitative evaluation of diffuse fibrosis.⁵ ECV shows association with cardiac dysfunction and the degree of myocardial fibrosis in AS^{6,7} and has been reported to be an independent predictor of mortality after AVR in severe AS.⁸

Contrast-enhanced computed tomography (CT) can be an alternative approach to CMR for measuring ECV, because of technological advances in CT, such as dual-energy CT, and technical improvement of CT scanning methods based on the pharmacokinetics of iodinated contrast materials.⁹ Recent studies have suggested that ECV can be successfully measured using single-energy as well as dual-energy CT, with good agreement with CMR findings.^{10–14} Furthermore, particularly in candidates for transcatheter AVR (TAVR), CT is more useful for evaluating ECV than CMR, because it can be measured by simply adding delayed myocardial enhancement imaging to the routine preprocedural CT used for assessing the anatomical suitability for TAVR.¹⁵ Accordingly, CT assessment of ECV may facilitate risk stratification and prognostic prediction in TAVR candidates.

Currently, there are no data on the prognostic value of CT-based ECV measurement in patients with severe AS. Thus, this study measured ECV in dual-energy CT for TAVR planning in patients with severe AS and evaluated the association between ECV and post-AVR clinical outcomes.

METHODS

The data that support the findings of this study are available from the corresponding author on reasonable request.

Study Design

This single-center cohort study retrospectively enrolled consecutive patients with severe AS who underwent CT angiography for TAVR planning between January 2015 and March 2018 at Kobe University Hospital. Patients underwent TAVR or surgical AVR (SAVR) after comprehensive clinical evaluation by a designated heart team following established guidelines. The following exclusion criteria were used: inadequate image quality attributable to artefacts and underuse of contrast agents attributable to advanced renal failure.

The study protocol adhered to the tenets of the 1975 Declaration of Helsinki. We provided patients with an appropriate opportunity to decline consent under the opt-out method on the institutional website; the requirement for written informed consent was waived. The study was approved by the institutional ethical committee of Kobe University Graduate School of Medicine.

CT Image Acquisition and Analysis

All image acquisitions were performed using a commercially available third-generation dual-source CT scanner (SOMATOM Force, Siemens Healthcare,

Forchheim, Germany). First, a noncontrast prospective electrocardiographic triggering CT scan for calcium scoring was performed with the following parameters at cardiac phase of 65%: collimation, 104–192×0.6 mm; tube voltage, 120 kV; and tube current, 80 mA. Images for calcium scoring were reconstructed with a 3-mm slice thickness. Next, standard electrocardiographic-triggering CT angiography for TAVR planning was performed using 12 mL of contrast agent (Iopamiron 370, 370 mg/mL; Bayer Yakuhin, Osaka, Japan) to assess the contrast agent transit time, using 0.6 mL/kg of contrast agent at a flow rate of 0.06 mL/kg per second, followed by 0.6 mL/kg diluted contrast (1:1; contrast/physiological saline) at the same flow rate used for angiography.¹⁵ Delayed enhancement image acquisition was performed 5 minutes after CT angiography, using a prospective electrocardiographic-triggering dual-energy scan with the following parameters: cardiac phase, 25% systole; collimation, 128×0.6 mm; tube voltage and current, 90/150 kV, with tin filtration and 250/192 mA/rotation; gantry rotation time, 250 ms; and pitch factor, 0.15. The axial image data were reconstructed using the following parameters: slice thickness, 1 mm; slice interval, 1 mm; and field of view, 240 mm. Delayed enhancement image was obtained routinely in the patients who underwent CT angiography for pre-TAVR assessment. β -Blockers and/or nitrates were not routinely used for premedication, because of hemodynamic concerns in severe AS. Aortic valve calcium score was measured on a commercially available workstation (Ziostation2 version 2.4.2.3, Ziosoft Inc, Tokyo, Japan) using the Agatston method and was expressed in arbitrary units.¹⁶

ECV Measurement

ECV was measured on a commercially available workstation (syngo.via VB10A, Siemens Healthcare, Forchheim, Germany). Iodine maps were obtained from 150-kV (with tin filtration) and 90-kV images on the workstation by using postprocessing software (heart PBV, Siemens Healthcare), based on the 3-material decomposition method (Figure 1A through 1C).¹⁷ After the iodine map images were reformatted to the short-axis plane with 5-mm section thickness, regions of interest were manually drawn on the myocardium, according to the American Heart Association's 16-segment model of the left ventricle, to measure the iodine density in the myocardium (Figure 1D). A circular region of interest (at least 100 mm²) was drawn in the left ventricular (LV) cavity to measure the iodine density in the blood pool. In iodine map images, iodine density was expressed in mg/mL. ECV was calculated using the following equation: $ECV (\%) = (1 - \text{hematocrit}) \times (\text{iodine density in myocardium}) / (\text{iodine density in blood pool}) \times 100$.¹³

Echocardiographic Measurement

Commercially available echocardiography systems were used for this study. All parameters were measured using the current American Society of Echocardiography and European Association of Echocardiography guidelines.¹⁸ The LV ejection fraction (LVEF) was measured using the modified Simpson method. LV mass was calculated with the cube formula. The early diastolic transmitral flow velocity (E) was measured using pulsed-wave Doppler echocardiography. Spectral pulsed-wave Doppler-derived early diastolic mitral annular velocity (e') was obtained by averaging the septal and lateral mitral annular velocity, and the E/e' ratio was calculated. The peak aortic-jet velocity was measured using continuity-wave Doppler mode. The aortic valve mean gradient was determined by tracing the velocity-time integral of the transaortic valvar flow, which was measured by using continuous-wave Doppler mode. The aortic valvar orifice area was calculated by the continuity equation and then indexed to the body surface area. The low-flow, low-gradient subtype included both the classic and paradoxical low-flow, low-gradient subtype.¹⁹

Study End Point

The primary end point of this study was a composite outcome of all-cause death and hospitalization for heart failure after AVR. The secondary end points were all-cause death, cardiac death, or hospitalization for heart failure. A standard definition was used to examine clinical events related to hospitalization for heart failure.²⁰ Cardiac death was defined as death attributable to myocardial ischemia and infarction, heart failure, or cardiac arrest resulting from arrhythmia or unknown cause. Clinical events were assessed by review of electronic medical records, reports from family members, and telephone interviews. The first event (death or hospitalization for heart failure) in each patient served as the clinical end point of interest.

Statistical Analysis

The normality of data distribution of all continuous variables was assessed using the Shapiro-Wilk test. Continuous variables are expressed as means±SD or median (interquartile range [IQR]), as appropriate, and were compared using the Student *t*-test or the Mann-Whitney *U* test. Categorical variables are expressed as counts and percentages and were compared using χ^2 or Fisher exact tests. The correlation was evaluated by using the Pearson or Spearman correlation coefficient appropriately.

Twenty randomly chosen participants were used to evaluate intraobserver and interobserver reliabilities

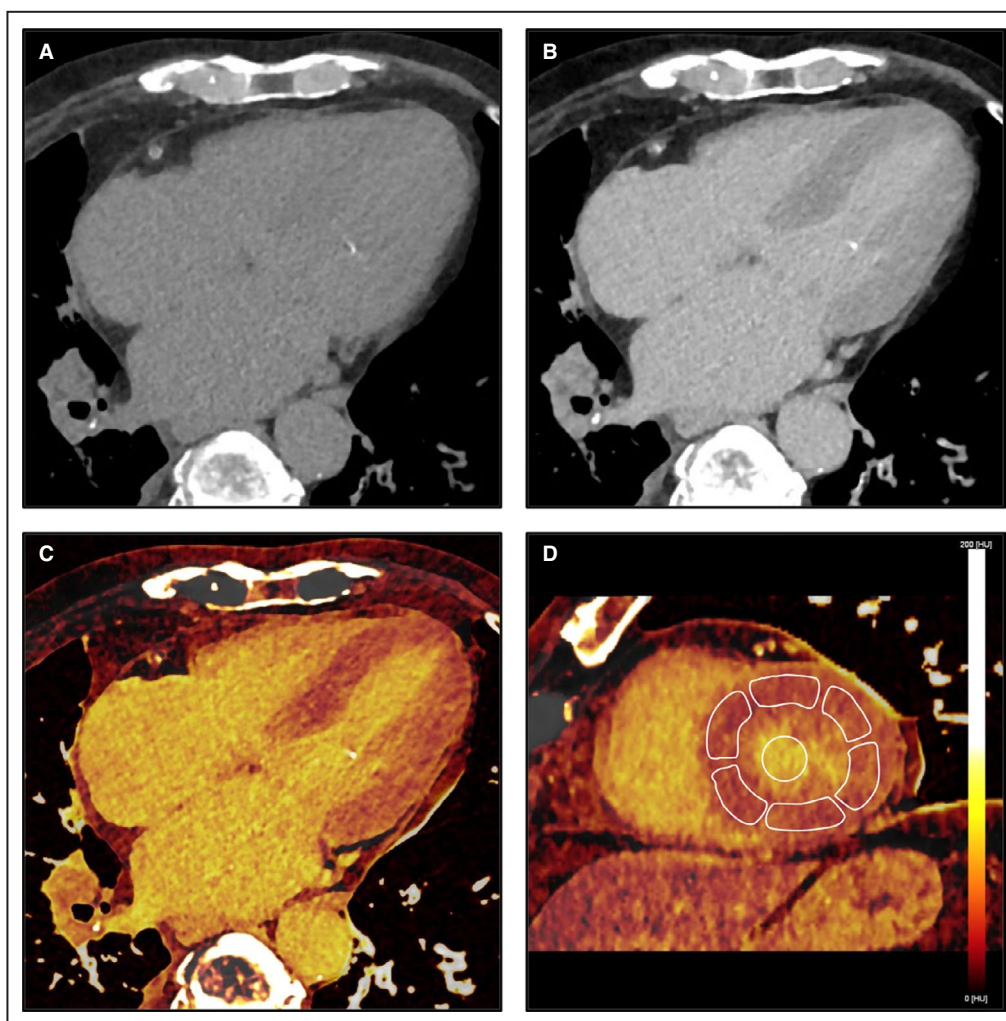


Figure 1. Methods for measuring extracellular volume fraction with dual-energy computed tomography.

On the basis of 150-kV (with tin filtration) (A) and 90-kV (B) delayed enhancement images, iodine maps (C) were obtained by using postprocessing software. After the iodine map images were reformatted to the short-axis plane (D), regions of interest (ROIs) were manually drawn on the myocardium, according to the American Heart Association's 16-segment model, to measure the iodine density in the myocardium. A circular ROI was drawn in the left ventricular cavity to measure the iodine density in the blood pool.

of ECV measurements using the intraclass correlation coefficient and Bland-Altman plot.

For the time-to-event analyses, cumulative incidence curves were constructed with the use of the Kaplan-Meier method, and the event rates were compared using the log-rank test. Competing-risk cumulative incidence method was used to estimate the cumulative risk of hospitalization for heart failure, and the Gray test was used to compare the study groups because death without evidence of hospitalization for heart failure was considered as a competing risk in the analysis. Univariable Cox regression analysis was performed to determine which variables were associated with the composite outcome. The significant variables on univariable analysis were included in the multivariable Cox regression model.

The statistical analyses were performed using JMP version 14.2.0 (SAS Institute, Cary, NC) and R version 3.6.3 (R Foundation for Statistical Computing, Vienna, Austria). $P < 0.05$ was considered statistically significant.

RESULTS

Study Population

A total of 147 patients with severe AS underwent CT angiography for TAVR planning during the study period. After excluding 33 patients who did not take the intervention for the aortic valve, we excluded 19 patients because of artefact-related inadequate image quality ($n=10$), low-contrast agent usage attributable to impaired renal function ($n=7$), or unavailable images

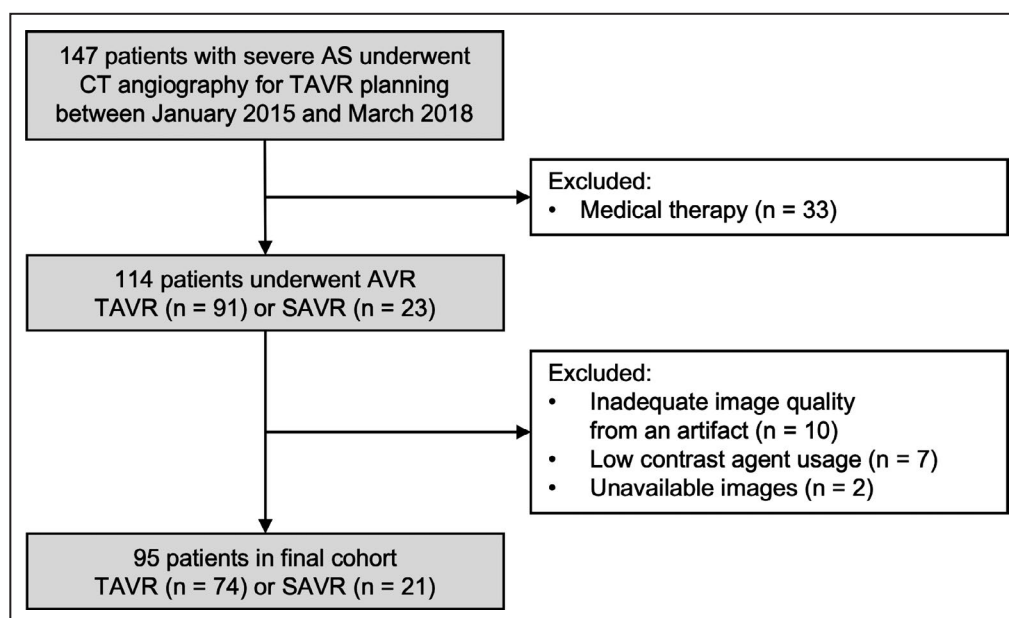


Figure 2. Flow diagram of study participants.

AS indicates aortic stenosis; AVR, aortic valve replacement; CT, computed tomography; SAVR, surgical AVR; and TAVR, transcatheter AVR.

($n=2$). Thus, 95 patients (mean age, 84.0 ± 5.0 years; 75% women) were studied (Figure 2). The median Society of Thoracic Surgeons Predicted Risk of Mortality (STS-PROM) score was 5.85% (IQR, 4.39%–9.43%). The proportions of patients who underwent TAVR and SAVR were 78% and 22%, respectively. In the subgroup analysis, the SAVR group had a higher STS-PROM score than the TAVR group (7.93% [IQR, 5.28%–11.88%] versus 5.67% [IQR, 4.33%–9.05%]; $P=0.049$) (Table S1).

ECV Assessment With Dual-Energy CT

Mean ECV was $28.1 \pm 3.8\%$. ECV data were normally distributed, with the mean approximately equal to the median (27.8%) (Figure 3). There is high variability in the number of patients clustering between 24% and 30% ECV values. The intraclass correlation coefficients for the intraobserver and interobserver measurements of the ECV were 0.965 and 0.930, respectively. In Bland-Altman plots, the mean intraobserver and interobserver differences were -0.19% (95% limit of agreement, -1.62% to 1.24%) and 0.40% (95% limit of agreement, -1.63% to 2.42%), respectively (Figure 4).

CT scans were performed at a median of 42 days (IQR, 18–69 days) before AVR. The median interval between the blood test and CT scan was 0 days (IQR, 0–3 days). At CT acquisition, the mean heart rate was 68 ± 14 beats/min. Mean effective radiation doses of dual-energy scans and mean contrast material volume per body weight were 4.7 ± 2.0 mSv and 0.93 ± 0.26 mL/kg, respectively.

Comparison of Patient Data between Low and High ECV

Patients were divided into low and high ECV groups, based on the median ECV (Table 1). Mean ECV was $25.2 \pm 2.0\%$ and $30.9 \pm 2.8\%$ in the low and high ECV groups, respectively ($P < 0.001$). Age and sex were similar in both groups. Body mass index and hematocrit values were significantly lower in the high ECV group, which also had a higher New York Heart Association class and B-type natriuretic peptide levels. Among the echocardiographic parameters, the high ECV group

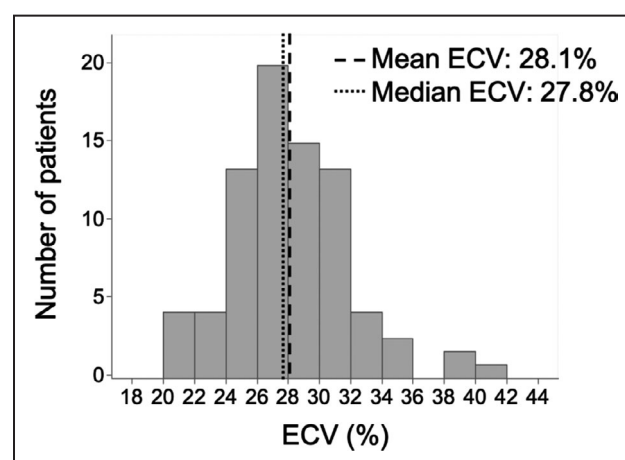


Figure 3. Histogram of extracellular volume fraction (ECV) distribution.

ECV was normally distributed, and the mean ($28.1 \pm 3.8\%$) and median (27.8%) ECV were almost equal.

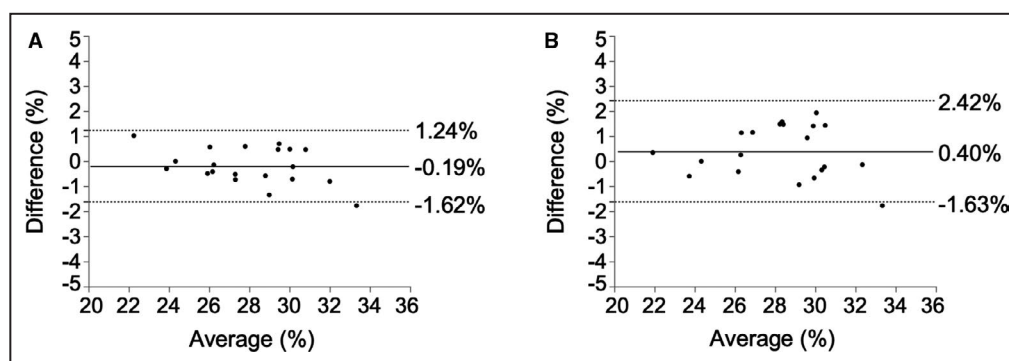


Figure 4. Bland-Altman plots showing intraobserver (A) and interobserver (B) reproducibility of extracellular volume fraction measurements.

The mean intraobserver and interobserver differences were -0.19% (95% limit of agreement, -1.62% to 1.24%) and 0.40% (95% limit of agreement, -1.63% to 2.42%), respectively.

had lower LVEF and higher E/e' . However, the 2 groups had similar echocardiographic measurements related to AS severity, such as transaortic valvar mean pressure gradient. There were no significant differences in the treatment approach.

Correlation of ECV With LV Decompensation and Severity of AS

Scattergrams indicating the correlation of ECV with measurements related to LV decompensation and AS severity are shown in Figure 5. ECV was significantly positively correlated with B-type natriuretic peptide ($r=0.395$; $P<0.001$) and the E/e' ratio ($r=0.223$; $P=0.038$) and negatively correlated with LVEF ($r=-0.251$; $P=0.014$) (Figure 5A through 5C). There was no significant correlation between ECV and echocardiographic parameters related to AS severity and the aortic valve calcium score (Figure 5D through 5F).

Relationship between ECV and Clinical Events

During a median follow-up of 2.6 years (IQR, 1.9–3.3 years) after AVR, 22 (23%) the composite outcome occurred, including 15 (16%) all-cause deaths, 6 (6%) cardiac deaths, and 11 (12%) hospitalizations for heart failure. Two deaths occurred within 30 days of AVR. In Kaplan-Meier analysis, the high ECV group had significantly higher rates of all-cause mortality and hospitalizations for heart failure than the low ECV group ($P=0.012$) (Figure 6A). All-cause mortality was significantly higher in the high than in the low ECV group ($P=0.009$) (Figure 6B). Cardiac death and hospitalization for heart failure occurred more frequently in the high ECV group, but this was not statistically significant ($P=0.078$ and $P=0.11$, respectively) (Figure 6C and 6D). In the univariable analysis, New York Heart Association class III or IV, atrial fibrillation, and ECV were significantly associated with the composite

outcomes (Table 2). In the multivariable Cox regression analysis, only ECV was independently associated with the composite outcomes (hazards ratio, 1.25; 95% CI, 1.10–1.41; $P<0.001$). In the subgroup analysis between TAVR and SAVR groups, ECV in each group was also significantly associated with the composite outcomes (Tables S2 and S3).

DISCUSSION

In the current study, we measured ECV using the iodine-density method with delayed enhancement dual-energy CT images. We demonstrated significant correlation of ECV with laboratory and echocardiographic findings related to LV decompensation, as well as significant association between ECV and clinical outcomes in patients with severe AS who underwent AVR. Furthermore, ECV was the only independent predictor of all-cause death and hospitalization for heart failure.

ECV Measurement Using Dual-Energy CT

Recent research studies have suggested that contrast-enhanced CT can be an alternative to CMR for measuring ECV.^{10–14} Although CMR is a well-established modality for evaluating ECV and produces excellent soft tissue contrast without radiation exposure, it has several limitations, such as a longer acquisition time, limited scan slices, and contraindication, in patients with claustrophobia or implanted pacemaker. Meanwhile, contrast-enhanced CT, although it requires some radiation exposure, has high spatial and temporal resolutions; besides, the soft tissue contrast has improved because of advancements in CT scanners and scanning methods. Particularly in TAVR candidates, ECV can be measured by simply adding a dual-energy CT image during routine acquisition of delayed enhancement preprocedural CT images, with

Table 1. Patient Characteristics

Characteristics	All patients	Low ECV group	High ECV group	P value
	(n=95)	(n=47)	(n=48)	
Age, y	84.0±5.0	84.5±4.3	83.5±5.6	0.34
Female sex, n (%)	71 (75)	35 (74)	36 (75)	0.95
Body mass index, kg/m ²	22.6±3.8	23.6±3.6	21.5±3.7	0.006*
Body surface area, m ²	1.42±0.16	1.44±0.17	1.40±0.16	0.23
Clinical status				
NYHA class III or IV	30 (32)	8 (17)	22 (46)	0.002*
STS-PROM score, %	5.85 (4.39–9.43)	5.67 (4.22–9.24)	6.45 (4.49–9.89)	0.58
Medical history, n (%)				
Hypertension	70 (74)	38 (81)	32 (67)	0.11
Dyslipidemia	35 (37)	20 (43)	15 (31)	0.25
Diabetes	20 (21)	10 (21)	10 (21)	0.96
Chronic kidney disease	39 (41)	19 (40)	20 (42)	0.90
Atrial fibrillation	16 (17)	6 (13)	10 (21)	0.29
Previous PCI	20 (21)	8 (17)	12 (25)	0.34
Previous CABG	2 (2)	1 (2)	1 (2)	0.99
Previous myocardial infarction	5 (5)	1 (2)	4 (8)	0.16
Implantable cardiac device	2 (2)	1 (2)	1 (2)	0.99
Blood examination findings				
Hematocrit, %	35.3±4.5	36.2±4.2	34.4±4.6	0.047*
Creatinine, mg/dL	0.85 (0.68–1.01)	0.87 (0.69–1.06)	0.84 (0.68–1.00)	0.63
eGFR, mL/min/1.73 m ²	54.6±16.4	53.2±16.1	56.0±16.8	0.41
BNP, pg/mL	268.5 (105.1–512.7)	159.6 (70.9–308.6)	358.7 (201.1–655.7)	<0.001*
Echocardiographic measures				
LV end-diastolic volume, mL	69.9 (53.4–89.5)	69.7 (52.0–88.3)	70.2 (53.8–95.2)	0.54
LV end-systolic volume, mL	24.4 (18.0–36.6)	23.5 (17.0–34.7)	26.7 (19.4–38.8)	0.19
LVEF, %	63.9 (56.0–71.0)	67.0 (60.6–72.0)	61.5 (52.3–69.8)	0.049*
LV mass, g	163.0 (136.4–211.7)	152.6 (136.4–193.7)	175.0 (132.4–231.3)	0.26
E/e' ratio	23.1 (16.3–30.9)	21.2 (15.7–29.2)	25.6 (17.6–33.8)	0.036*
Peak aortic-jet velocity, cm/s	451.0 (425.8–491.1)	449.5 (425.8–492.4)	459.1 (421.8–490.7)	0.95
Mean aortic valve gradient, mm Hg	51.4±13.4	51.5±13.2	51.4±13.8	0.97
Aortic valve area, cm ²	0.61±0.16	0.62±0.14	0.59±0.19	0.27
Indexed aortic valve area, cm ² /m ²	0.43±0.11	0.44±0.10	0.42±0.13	0.53
Bicuspid aortic valve, n (%)	7 (7)	3 (6)	4 (8)	0.72
Low-flow, low-gradient subtype, n (%)	9 (9)	3 (6)	6 (13)	0.30
CT measures				
ECV, %	28.1±3.8	25.2±2.0	30.9±2.8	<0.001*
Aortic valve calcium score, AU	2307.1 (1659.4–3308.9)	2307.1 (1550.0–3259.0)	2296.3 (1703.4–3376.5)	0.69
Intervention for aortic valve, n (%)				
SAVR	21 (22)	12 (26)	9 (19)	0.43
TAVR	74 (78)	35 (74)	39 (81)	

Continuous variables are expressed as mean±SD or median (interquartile range) and were compared using the Student *t*-test or the Mann-Whitney *U* test, as appropriate. Categorical variables are expressed as counts and percentages and were compared using χ^2 or Fisher exact tests. AU indicates Agatston unit; BNP, B-type natriuretic peptide; CABG, coronary artery bypass grafting; CT, computed tomography; E, early diastolic transmitral flow velocity; e', early diastolic mitral annular velocity; ECV, extracellular volume fraction; eGFR, estimated glomerular filtration rate; LV, left ventricular; LVEF, LV ejection fraction; NYHA, New York Heart Association; PCI, percutaneous coronary intervention; SAVR, surgical aortic valve replacement; STS-PROM, Society of Thoracic Surgeons Predicted Risk of Mortality; and TAVR, transcatheter aortic valve replacement.

**P*<0.05.

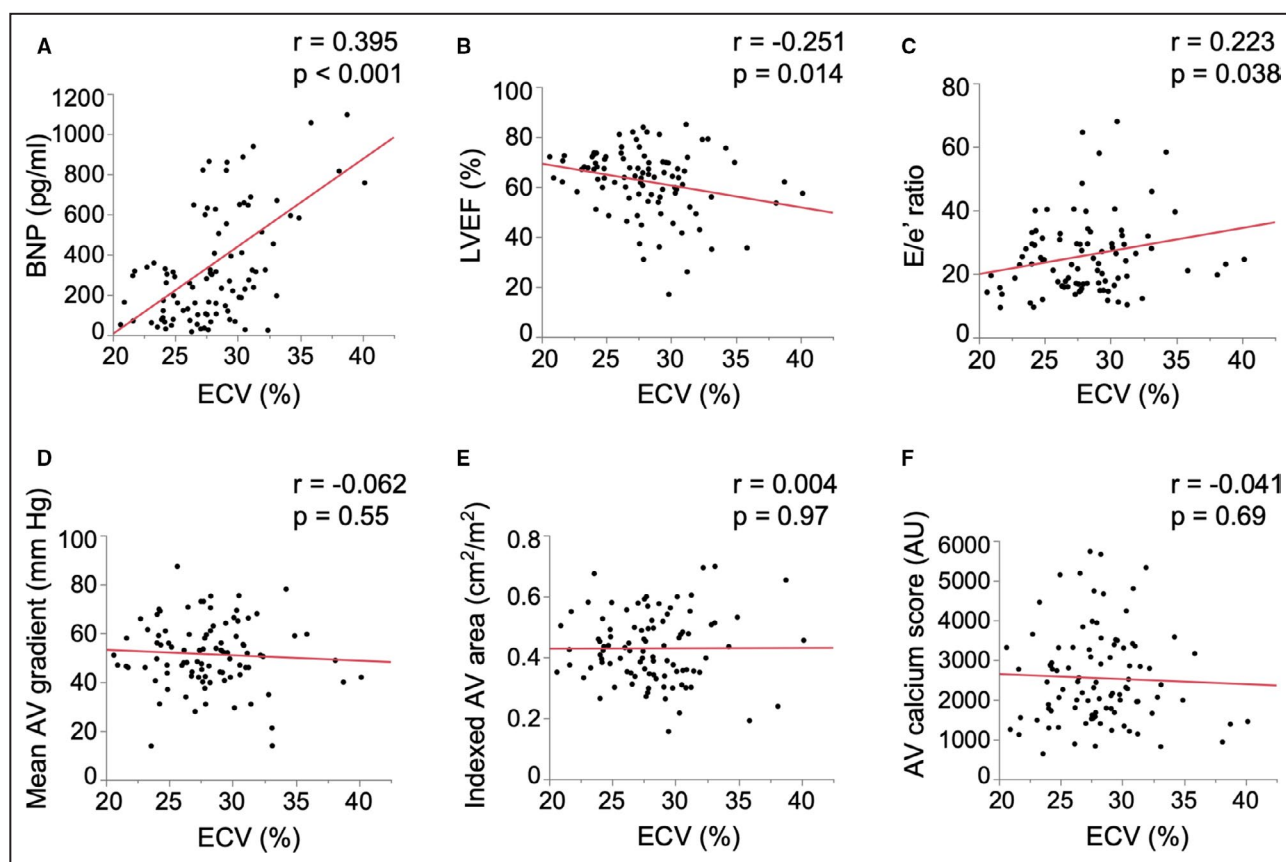


Figure 5. Scattergram indicating correlation of extracellular volume fraction (ECV) with B-type natriuretic peptide (BNP) (A), left ventricular ejection fraction (LVEF) (B), early diastolic transmitral flow velocity (E)/early diastolic mitral annular velocity (e') ratio (C), mean aortic valve (AV) gradient (D), indexed AV area (E), and AV calcium score (F).

BNP, LVEF, and E/e' ratio were significantly correlated with ECV, whereas there was no significant correlation between ECV and parameters related to aortic stenosis severity. AU indicates Agatston unit.

low additional radiation (4.7 ± 2.0 mSv). It may be appropriate for elderly patients with severe AS who tend not to tolerate CMR because of the long acquisition times and long breath holds. Actually, a few studies have evaluated ECV measured with additional delayed enhancement images on routine preprocedural TAVR-planning CT,^{21,22} and found mean ECV values in patients with severe AS of 28% to 32%, similar to our results.

There are 2 methods for ECV measurement by CT: the subtraction method, using single-energy CT, and the iodine-density method, using dual-energy CT. The subtraction method is a previously validated standard method that requires precontrast and postcontrast equilibrium phase images. This method enables both single- and dual-energy CT scanners to evaluate ECV. However, differentiating between the myocardium and blood on precontrast CT images is challenging, leading to misregistration of precontrast and postcontrast images. In contrast, the iodine-density method uses only the equilibrium-phase iodine density images

generated by dual-energy CT images. These images show the spread of iodine in a voxel at a state of equilibrium, and ECV can be measured without the need for precontrast images. We measured ECV using the iodine-density method with delayed enhancement dual-energy CT images and found the method to be highly reproducible (interobserver intraclass correlation coefficient, 0.930). The iodine-density method can reduce radiation dose because it alleviates the need for precontrast images.²³ Moreover, dual-energy CT allows improvement in the signal/noise ratio by using virtual monoenergetic images and iodine maps compared with single-energy CT.^{24,25} In addition, the iodine-density method is reportedly more reliable as a diagnostic modality for myocardial fibrosis.¹⁴ Emoto et al measured ECV using 2 CT-based methods and compared these measurements with the CMR method. The iodine-density method was more accurate than the subtraction method, using CMR as the reference standard method. Therefore, we adopted the iodine-density method in dual-energy CT in the current study.

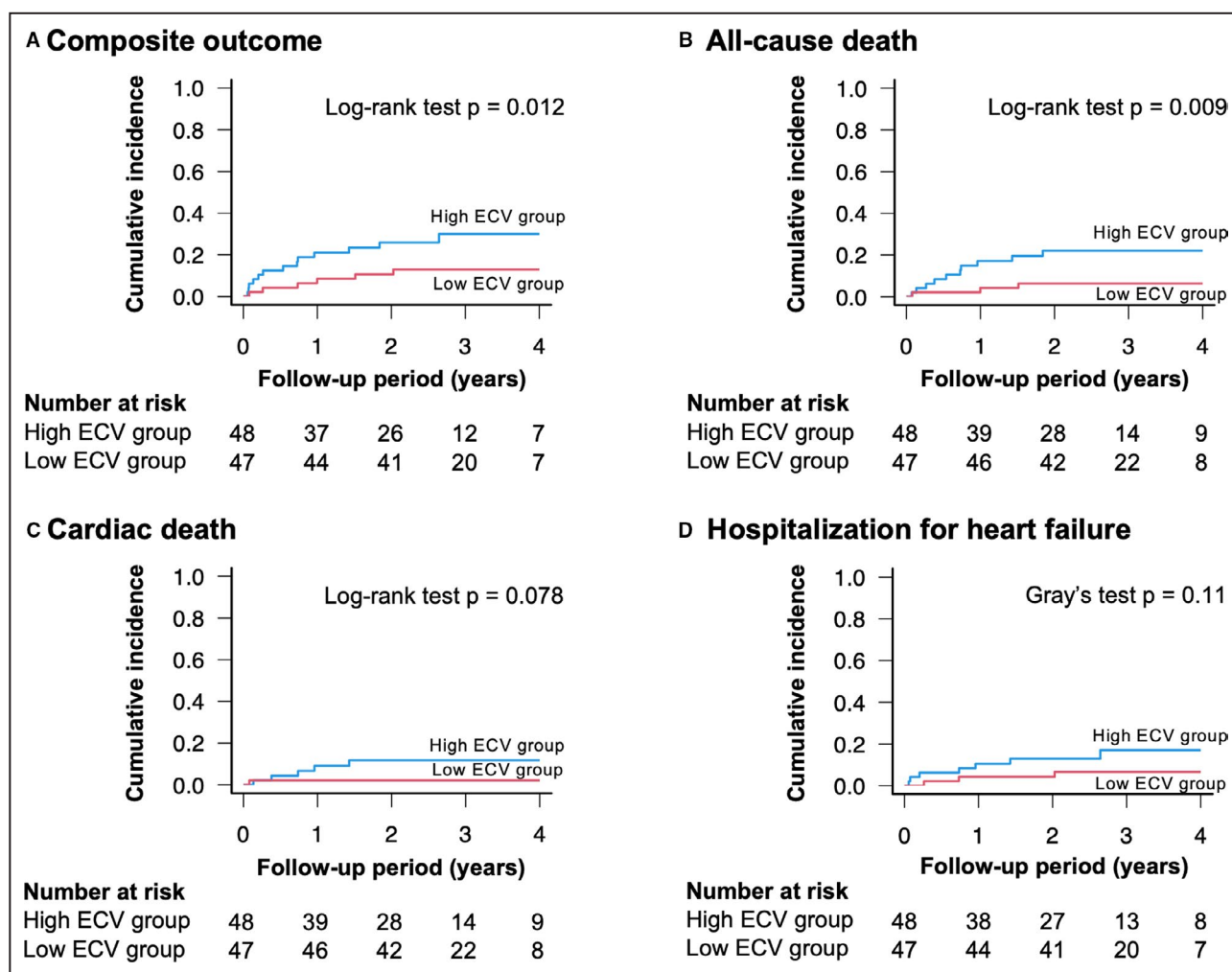


Figure 6. Cumulative incidence curves between the low and high extracellular volume fraction (ECV) groups.

The high ECV group had significantly higher rates of the composite outcomes of all-cause death and hospitalization for heart failure ($P=0.012$) (A) and higher rates of all-cause death ($P=0.009$) (B). Cardiac death and hospitalization for heart failure occurred more frequently in the high ECV group, although this was not statistically significant ($P=0.078$ and $P=0.11$, respectively) (C and D).

Clinical Significance of ECV Assessment

In the present study, ECV measured with CT was significantly associated with New York Heart Association class and B-type natriuretic peptide. Similarly, several studies showed that ECV measured with CMR correlated positively with NT-proBNP (N-terminal pro-B-type natriuretic peptide) and was significantly associated with clinical symptoms, expressed as New York Heart Association class and 6-minute walk test distance, in patients with severe AS.^{8,26} Furthermore, we demonstrated that ECV and echocardiographic measurements of LVEF and the E/e' ratio, indicating both systolic and diastolic dysfunction, correlated significantly. Previous studies have reported that higher ECV measured with CMR was significantly associated with lower LVEF and higher E/e' ratio in patients with severe AS,^{6,8} in agreement with our study results. Taken together, these findings imply that ECV could

be a composite marker indicating both hormonal and hemodynamic abnormalities in patients with AS.

Interestingly, ECV measured with CT was not significantly associated with the severity of AS, as determined in transthoracic echocardiogram and CT. Several clinical studies have suggested that ECV measured with CMR was not associated with echocardiographic parameters, reflecting the severity of AS in patients undergoing AVR.^{6,8} The authors speculated that this is because AS progression leads to myocardial fibrosis and LV dysfunction, which decrease the aortic valve pressure gradient. However, this cannot explain the lack of significant correlation between ECV and the aortic valve calcium score in the current study. This score, the gold standard for evaluating the severity of low-flow, low-gradient AS, was reported to be significantly associated with the severity of AS, irrespective of cardiac systolic function.²⁷ To date, no association

Table 2. Univariable and Multivariable Cox Regression Analysis for Composite Outcome

Characteristics	Univariable analysis			Multivariable analysis		
	HR	95% CI	P value	HR	95% CI	P value
Age, y	1.03	0.94–1.13	0.55			
Male sex	1.30	0.53–3.19	0.58			
Body mass index, kg/m ²	0.90	0.79–1.01	0.071			
NYHA class III or IV	2.79	1.20–6.46	0.019*	1.18	0.45–3.09	0.74
STS-PROM score, %	1.05	0.96–1.15	0.27			
Atrial fibrillation	2.89	1.18–7.11	0.032*	1.86	0.69–5.04	0.23
Coronary artery disease	0.72	0.28–1.84	0.48			
Implantable cardiac device	2.23	0.28–17.47	0.49			
BNP, pg/mL	1.00	0.99–1.00	0.073			
LVEF, %	0.99	0.96–1.02	0.50			
LV mass, g	1.00	0.99–1.01	0.81			
E/e' ratio	1.01	0.98–1.04	0.39			
Peak aortic-jet velocity, cm/s	1.00	0.99–1.01	0.61			
Mean aortic valve gradient, mm Hg	1.00	0.97–1.04	0.79			
Indexed aortic valve area, cm ² /m ²	7.30	0.19–289.6	0.28			
Bicuspid aortic valve	0.53	0.07–3.92	0.49			
Low-flow, low-gradient subtype	1.56	0.46–5.29	0.50			
ECV, %	1.29	1.15–1.44	<0.001*	1.25	1.10–1.41	<0.001*
Aortic valve calcium score, AU	1.00	0.99–1.00	0.58			
TAVR	1.95	0.61–6.22	0.23			

Univariable Cox regression analysis was performed to identify the variables that were associated with the composite outcome. Significant variables identified in the univariable analysis were included in the multivariable Cox regression model. Coronary artery disease defined as history of previous myocardial infarction, percutaneous coronary intervention, or coronary artery bypass grafting. AU indicates Agatston unit; BNP, B-type natriuretic peptide; CI, confidence interval; E, early diastolic transmitral flow velocity; e', early diastolic mitral annular velocity; ECV, extracellular volume fraction; HR, hazard ratio; LV, left ventricular; LVEF, LV ejection fraction; NYHA, New York Heart Association; STS-PROM, Society of Thoracic Surgeons Predicted Risk of Mortality; and TAVR, transcatheter aortic valve replacement.

* $P < 0.05$.

between ECV and the aortic valve calcium score has been reported. Given that the ECV is irrelevant to AS severity, our findings implied that the ECV might reflect cardiac impairment not only because of severe AS, but also because of unspecified cardiomyopathies, such as cardiac amyloidosis, hypertrophic cardiomyopathy, myocardial inflammation, and myocardial infarction, which elevate ECV by causing alterations in the extracellular component of the myocardium.⁵ In particular, cardiac amyloidosis is concomitantly observed in 14% to 16% of TAVR candidates.^{28,29} A recent article demonstrated that ECV derived from CT can detect dual AS-amyloid pathology in TAVR candidates.^{21,22} From this perspective, our results might suggest that patients with AS with higher ECV have a higher probability of concomitant cardiac amyloidosis, and thus a poor prognosis.

Prognostic Impact of ECV Measurement

ECV measured with CT was the only independent predictor of composite outcomes of all-cause death and hospitalization for heart failure in the present study. Histological studies reported that the degree of

myocardial fibrosis at the time of AVR was significantly associated with the degree of LV functional improvement and clinical outcomes, including mortality and symptoms of heart failure.^{2,30} In previous analysis of the association between CMR-determined ECV and adverse outcomes in patients with AS,^{6,31} ECV was closely related to all-cause death and heart failure, although it was not significant, because of relatively small sample sizes. More recently, Everett et al⁸ conducted an international multicenter study to evaluate the association between CMR-determined ECV and clinical outcomes after AVR in 440 patients with severe AS. They found that ECV was independently associated with all-cause mortality after AVR after adjustment for various well-established prognostic markers, including age, sex, and LVEF, consistent with our results. To the best of our knowledge, no previous investigation has demonstrated the significant association between ECV, measured by the iodine-density method using dual-energy CT, and clinical outcomes in patients with AS.

Notably, the STS-PROM score was not significantly associated with the primary end point. However, in the subgroup analysis, the STS-PROM score was

significantly associated with the primary end point in the SAVR group, although not in the TAVR group. The STS-PROM score is one of the well-established prognostic indicators following AVR. However, contrary to our findings, recent Japanese cohort studies have demonstrated that the STS-PROM score has predictive power for clinical outcomes in older Japanese patients treated with TAVR.^{32,33} In our study, we noted a higher incidence of primary end point in patients undergoing TAVR with high STS-PROM score, although this tendency was not statistically significant. If the sample size was larger, the STS-PROM score might have been significantly associated with the prognosis in patients who underwent TAVR. Further investigations with a larger sample size and longer follow-up period are required to establish a more robust prognostic prediction model.

Study Limitations

This study has several limitations. First, this was a single-center, retrospective study, and may have had selection bias, even though we enrolled patients consecutively. Second, the sample size was relatively small, attributable to which the statistical power was relatively low. To avoid type II errors, future studies must assess larger samples of patients. Third, the study population was limited to older, mainly female patients, affecting generalizability of our findings. Fourth, a single CT scanner vendor was used in the current study. The performance of ECV measured by using other CT vendors has not been assessed. Fifth, for the assessment of clinical events, we used reports from family members and telephone interviews in those patients who did not visit our institution for follow-up. Therefore, some recall bias may potentially have occurred. Finally, we did not screen other concomitant cardiomyopathies using imaging modalities such as CMR, scintigraphy, and myocardial biopsy, which may have caused ECV elevation.

CONCLUSIONS

Myocardial ECV using dual-energy CT was significantly associated with the composite outcomes of all-cause death and hospitalization for heart failure in patients with severe AS who underwent AVR. ECV measurements with CT obtained before AVR may be valuable for predicting prognosis in this population.

ARTICLE INFORMATION

Received December 22, 2020; accepted July 30, 2021.

Affiliations

Division of Cardiovascular Medicine, Department of Internal Medicine (M.S., T.T., Y.I., H.F., K.M., Y.T., H.T., H.K., H.O., H.T., S.F., K.H.); Department of Radiology (Y.W., A.K.K.) and Division of Cardiovascular Surgery, Department of Surgery, Kobe University Graduate School of Medicine, Japan, (K.O.).

Acknowledgments

We would like to thank Dr Tatsuya Nishii for helpful discussions. We are also grateful for the technical support provided by our radiological technologists: Asuka Sunakawa, Takuro Nishio, Tomoki Maebayashi, Akiyo Fukutomi, Kiyosumi Kagawa, and Noriyuki Negi.

Sources of Funding

None.

Disclosures

None.

Supplementary Material

Table S1–S3

REFERENCES

1. Dweck MR, Boon NA, Newby DE. Calcific aortic stenosis: a disease of the valve and the myocardium. *J Am Coll Cardiol*. 2012;60:1854–1863. doi: 10.1016/j.jacc.2012.02.093
2. Weidemann F, Herrmann S, Störk S, Niemann M, Frantz S, Lange V, Beer M, Gattenlöhner S, Voelker W, Ertl G, et al. Impact of myocardial fibrosis in patients with symptomatic severe aortic stenosis. *Circulation*. 2009;120:577–584. doi: 10.1161/CIRCULATIONAHA.108.847772
3. Milano AD, Faggian G, Dodonov M, Golia G, Tomezzoli A, Bortolotti U, Mazzucco A. Prognostic value of myocardial fibrosis in patients with severe aortic valve stenosis. *J Thorac Cardiovasc Surg*. 2012;144:830–837. doi: 10.1016/j.jtcvs.2011.11.024
4. Hein S, Arnon E, Kostin S, Schönburg M, Elsässer A, Polyakova V, Bauer EP, Klövekorn W-P, Schaper J. Progression from compensated hypertrophy to failure in the pressure-overloaded human heart: structural deterioration and compensatory mechanisms. *Circulation*. 2003;107:984–991. doi: 10.1161/01.CIR.0000051865.66123.B7
5. Messroghli DR, Moon JC, Ferreira VM, Grosse-Wortmann L, He T, Kellman P, Mascherbauer J, Nezafat R, Salerno M, Schelbert EB, et al. Clinical recommendations for cardiovascular magnetic resonance mapping of T1, T2, T2 and extracellular volume: a consensus statement by the Society for Cardiovascular Magnetic Resonance (SCMR) endorsed by the European Association for Cardiovascular Imaging. *J Cardiovasc Magn Reson*. 2017;19:1–24. doi: 10.1186/s12968-017-0389-8
6. Treibel TA, López B, González A, Menacho K, Schofield RS, Ravassa S, Fontana M, White SK, DiSalvo C, Roberts N, et al. Reappraising myocardial fibrosis in severe aortic stenosis: an invasive and non-invasive study in 133 patients. *Eur Heart J*. 2018;39:699–709. doi: 10.1093/eurheartj/ehx353
7. Park SJ, Cho SW, Kim SM, Ahn J, Carriere K, Jeong DS, Lee SC, Park SW, Choe YH, Park PW, et al. Assessment of myocardial fibrosis using multimodality imaging in severe aortic stenosis: comparison with histologic fibrosis. *JACC Cardiovasc Imaging*. 2019;12:109–119. doi: 10.1016/j.jcmg.2018.05.028
8. Everett RJ, Treibel TA, Fukui M, Lee H, Rigolli M, Singh A, Bijsterveld P, Tastet L, Musa TA, Dobson L, et al. Extracellular myocardial volume in patients with aortic stenosis. *J Am Coll Cardiol*. 2020;75:304–316. doi: 10.1016/j.jacc.2019.11.032
9. Allard M, Doucet D, Kien P, Bonnemain B, Caillé JM. Experimental study of DOTA-gadolinium pharmacokinetics and pharmacologic properties. *Invest Radiol*. 1988;23:S271–S274. doi: 10.1097/00004424-198809001-00059
10. Treibel TA, Bandula S, Fontana M, White SK, Gilbertson JA, Herrey AS, Gillmore JD, Punwani S, Hawkins PN, Taylor SA, et al. Extracellular volume quantification by dynamic equilibrium cardiac computed tomography in cardiac amyloidosis. *J Cardiovasc Comput Tomogr*. 2015;9:585–592. doi: 10.1016/j.jcct.2015.07.001
11. Lee HJ, Im DJ, Youn JC, Chang S, Suh YJ, Hong YJ, Kim YJ, Hur J, Choi BW. Myocardial extracellular volume fraction with dual-energy equilibrium contrast-enhanced cardiac CT in nonischemic cardiomyopathy: a prospective comparison with cardiac MR imaging. *Radiology*. 2016;280:49–57. doi: 10.1148/radiol.2016151289
12. Ohta Y, Kishimoto J, Kitao S, Yunaga H, Mukai-Yatagai N, Fujii S, Yamamoto K, Fukuda T, Ogawa T. Investigation of myocardial extracellular volume fraction in heart failure patients using iodine map with rapid-kV switching dual-energy CT: segmental comparison with MRI

- T1 mapping. *J Cardiovasc Comput Tomogr*. 2019;14:349–355. doi: 10.1016/j.jcct.2019.12.032
13. Abadia AF, van Assen M, Martin SS, Vingiani V, Griffith LP, Giovagnoli DA, Bauer MJ, Schoepf UJ. Myocardial extracellular volume fraction to differentiate healthy from cardiomyopathic myocardium using dual-source dual-energy CT. *J Cardiovasc Comput Tomogr*. 2019;14:162–167. doi: 10.1016/j.jcct.2019.09.008
 14. Emoto T, Oda S, Kidoh M, Nakaura T, Nagayama Y, Sakabe D, Kakei K, Goto M, Funama Y, Hatemura M, et al. Myocardial extracellular volume quantification using cardiac computed tomography: a comparison of the dual-energy iodine method and the standard subtraction method. *Acad Radiol*. 2021;28:e119–e126. doi: 10.1016/j.acra.2020.03.019
 15. Blanke P, Weir-McCall JR, Achenbach S, Delgado V, Hausleiter J, Jilalawi H, Marwan M, Norgaard BL, Piazza N, Schoenhagen P, et al. Computed tomography imaging in the context of transcatheter aortic valve implantation (TAVI)/transcatheter aortic valve replacement (TAVR): an expert consensus document of the society of cardiovascular computed tomography. *J Cardiovasc Comput Tomogr*. 2019;13:1–20. doi: 10.1016/j.jcct.2018.11.008
 16. Agatston AS, Janowitz WR, Hildner FJ, Zusmer NR, Viamonte M, Detrano R. Quantification of coronary artery calcium using ultrafast computed tomography. *J Am Coll Cardiol*. 1990;15:827–832. doi: 10.1016/0735-1097(90)90282-T
 17. Johnson TRC, Krauß B, Sedlmair M, Grasruck M, Bruder H, Morhard D, Fink C, Weckbach S, Lenhard M, Schmidt B, et al. Material differentiation by dual energy CT: initial experience. *Eur Radiol*. 2007;17:1510–1517. doi: 10.1007/s00330-006-0517-6
 18. Lang RM, Badano LP, Mor-Avi V, Afilalo J, Armstrong A, Ernande L, Flachskampf FA, Foster E, Goldstein SA, Kuznetsova T, et al. Recommendations for cardiac chamber quantification by echocardiography in adults: an update from the American Society of Echocardiography and the European Association of Cardiovascular Imaging. *J Am Soc Echocardiogr*. 2015;28:1–39. doi: 10.1016/j.echo.2014.10.003
 19. Baumgartner H, Hung J, Bermejo J, Chambers JB, Edvardsen T, Goldstein S, Lancellotti P, LeFebvre M, Miller F, Otto CM. Recommendations on the echocardiographic assessment of aortic valve stenosis: a focused update from the European Association of Cardiovascular Imaging and the American Society of Echocardiography. *J Am Soc Echocardiogr*. 2017;30:372–392. doi: 10.1016/j.echo.2017.02.009
 20. Kappetein AP, Head SJ, G  n  reux P, Piazza N, van Mieghem NM, Blackstone EH, Brott TG, Cohen DJ, Cutlip DE, van Es G-A, et al. Updated standardized endpoint definitions for transcatheter aortic valve implantation: the Valve Academic Research Consortium-2 consensus document. *Eur Heart J*. 2012;33:2403–2418. doi: 10.1093/eurheartj/ehs255
 21. Scully PR, Patel KP, Saberwal B, Klotz E, Augusto JB, Thornton GD, Hughes RK, Manisty C, Lloyd G, Newton JD, et al. Identifying cardiac amyloid in aortic stenosis ECV quantification by CT in TAVR patients. *JACC Cardiovasc Imaging*. 2020;13:2177–2189. doi: 10.1016/j.jcmg.2020.05.029
 22. Oda S, Kidoh M, Takashio S, Inoue T, Nagayama Y, Nakaura T, Shiraishi S, Tabata N, Usuku H, Kaikita K, et al. Quantification of myocardial extracellular volume with planning computed tomography for transcatheter aortic valve replacement to identify occult cardiac amyloidosis in patients with severe aortic stenosis. *Circ Cardiovasc Imaging*. 2020;13:e010358. doi: 10.1161/CIRCIMAGING.119.010358
 23. van Assen M, De Cecco CN, Sahbaee P, Eid MH, Griffith LP, Bauer MJ, Savage RH, Varga-Szemes A, Oudkerk M, Vliegenthart R, et al. Feasibility of extracellular volume quantification using dual-energy CT. *J Cardiovasc Comput Tomogr*. 2019;13:81–84. doi: 10.1016/j.jcct.2018.10.011
 24. Scheske JA, O'Brien JM, Earls JP, Min JK, LaBounty TM, Cury RC, Lee T-Y, So A, Hague CJ, Al-Hassan D, et al. Coronary artery imaging with single-source rapid kilovolt peak-switching dual-energy CT. *Radiology*. 2013;268:702–709. doi: 10.1148/radiol.13121901
 25. Matsumoto K, Jinzaki M, Tanami Y, Ueno A, Yamada M, Kuribayashi S. Virtual monochromatic spectral imaging with fast kilovoltage switching: improved image quality as compared with that obtained with conventional 120-kVp CT. *Radiology*. 2011;259:257–262. doi: 10.1148/radiol.11100978
 26. Flett AS, Sado DM, Quarta G, Mirabel M, Pellerin D, Herrey AS, Hausenloy DJ, Ariti C, Yap J, Kolvekar S, et al. Diffuse myocardial fibrosis in severe aortic stenosis: an equilibrium contrast cardiovascular magnetic resonance study. *Eur Heart J Cardiovasc Imaging*. 2012;13:819–826. doi: 10.1093/ehjci/jes102
 27. Aggarwal SR, Clavel MA, Messika-Zeitoun D, Cuffe C, Malouf J, Araoz PA, Mankad R, Michelena H, Vahanian A, Enriquez-Sarano M. Sex differences in aortic valve calcification measured by multidetector computed tomography in aortic stenosis. *Circ Cardiovasc Imaging*. 2013;6:40–47. doi: 10.1161/CIRCIMAGING.112.980052
 28. Scully PR, Treibel TA, Fontana M, Lloyd G, Mullen M, Pugliese F, Hartman N, Hawkins PN, Menezes LJ, Moon JC. Prevalence of cardiac amyloidosis in patients referred for transcatheter aortic valve replacement. *J Am Coll Cardiol*. 2018;71:463–464. doi: 10.1016/j.jacc.2017.11.037
 29. Casta  o A, Narotsky DL, Hamid N, Khaliq OK, Morgenstern R, DeLuca A, Rubin J, Chiuzan C, Nazif T, Vahl T, et al. Unveiling transthyretin cardiac amyloidosis and its predictors among elderly patients with severe aortic stenosis undergoing transcatheter aortic valve replacement. *Eur Heart J*. 2017;38:2879–2887. doi: 10.1093/eurheartj/ehx350
 30. Azevedo CF, Nigri M, Higuchi ML, Pomerantzeff PM, Spina GS, Sampaio RO, Tarasoutchi F, Grinberg M, Rochitte CE. Prognostic significance of myocardial fibrosis quantification by histopathology and magnetic resonance imaging in patients with severe aortic valve disease. *J Am Coll Cardiol*. 2010;56:278–287. doi: 10.1016/j.jacc.2009.12.074
 31. Nadjiri J, Nieberler H, Hendrich E, Will A, Pellegrini C, Husser O, Hengstenberg C, Greiser A, Martinoff S, Hadamitzky M. Prognostic value of T1-mapping in TAVR patients: extra-cellular volume as a possible predictor for peri- and post-TAVR adverse events. *Int J Cardiovasc Imaging*. 2016;32:1625–1633. doi: 10.1007/s10554-016-0948-3
 32. Sawa Y, Takayama M, Goto T, Takanashi S, Komiya T, Tobaru T, Maeda K, Kuratani T, Sakata Y. Five-Year Outcomes of the First Pivotal Clinical Trial of Balloon-Expandable Transcatheter Aortic Valve Replacement in Japan (PREVAIL JAPAN). *Circ J*. 2017;81:1102–1107. doi: 10.1253/circj.CJ-17-0111
 33. Ishizu K, Shirai S, Isotani A, Hayashi M, Kawaguchi T, Taniguchi T, Ando K, Yashima F, Tada N, Yamawaki M, et al. Long-term prognostic value of the society of thoracic surgery risk score in patients undergoing transcatheter aortic valve implantation (from the OCEAN-TAVI Registry). *Am J Cardiol*. 2021;149:86–94. doi: 10.1016/j.amjcard.2021.03.027

SUPPLEMENTAL MATERIAL

Table S1. Patient characteristics between TAVR and SAVR groups.

	TAVR group (n = 74)	SAVR group (n = 21)	p Value
Age, years	85.0 ± 4.1	80.5 ± 6.2	<0.001
Female, n (%)	57 (77)	14 (67)	0.35
Body mass index, kg/m ²	22.7 ± 4.0	22.2 ± 2.9	0.58
Body surface area, m ²	1.41 ± 0.16	1.43 ± 0.17	0.73
Clinical status			
NYHA class III or IV	26 (35)	4 (19)	0.15
STS-PROM score, %	5.67 (4.33–9.05)	7.93 (5.28–11.88)	0.049
Past medical history			
Hypertension, n (%)	52 (70)	18 (86)	0.14
Dyslipidemia, n (%)	26 (35)	9 (43)	0.52
Diabetes mellitus, n (%)	14 (19)	6 (29)	0.35
Chronic kidney disease, n (%)	29 (39)	10 (48)	0.49
Atrial fibrillation, n (%)	13 (18)	3 (14)	0.72
Previous PCI, n (%)	18 (24)	2 (10)	0.12
Previous CABG, n (%)	2 (3)	0 (0)	0.31
Previous myocardial infarction, n (%)	5 (7)	0 (0)	0.11
Implantable cardiac device, n (%)	0 (0)	2 (10)	0.013
Blood exams			
Hematocrit, %	35.0 ± 4.4	36.5 ± 4.8	0.18
Creatinine, mg/dl	0.83 (0.68–1.04)	0.88 (0.74–0.98)	0.66
eGFR, ml/min/1.73m ²	54.8 ± 17.1	53.9 ± 13.8	0.83
BNP, pg/ml	292.4 (121.9–523.1)	159.4 (82.3–550.3)	0.28
Echocardiographic measures			
LV end-diastolic volume, ml	69.7 (54.6–88.7)	72.0 (50.2–92.5)	0.99
LV end-systolic volume, ml	24.2 (18.7–35.7)	24.7 (15.0–38.7)	0.95
LVEF, %	63.7 (56.0–70.6)	67.1 (54.6–71.7)	0.63
LV mass, g	164.5 (139.7–214.7)	149.5 (124.5–218.3)	0.56
E/e' ratio	23.1 (16.8–29.4)	23.1 (14.8–39.9)	0.77

Peak aortic-jet velocity, cm/s	450.3 (426.9–488.1)	456.9 (413.5–545.3)	0.74
Mean aortic valve gradient, mm Hg	51.5 ± 12.1	51.3 ± 17.7	0.96
Aortic valve area, cm ²	0.61 ± 0.15	0.59 ± 0.21	0.59
Indexed aortic valve area, cm ² /m ²	0.43 ± 0.11	0.41 ± 0.14	0.44
Bicuspid aortic valve, n (%)	2 (3)	5 (24)	0.004
Low-flow, low-gradient subtype, n (%)	6 (8)	3 (14)	0.41
CT measures			
ECV, %	28.3 ± 3.9	27.4 ± 3.2	0.36
Aortic valve calcium score, AU	2293.6 (1569.2– 3305.6)	2378.3 (1928.8– 3311.0)	0.72
Clinical events			0.43
Composite outcome*, n (%)	18 (24)	4 (19)	0.61
All-cause death, n (%)	13 (18)	2 (10)	0.35
Cardiac death, n (%)	5 (7)	1 (5)	0.73
Hospitalization for heart failure, n (%)	9 (12)	2 (10)	0.73

Values are mean ± standard deviation, n (%), or median (interquartile range). *Composite outcome defined as all-cause death or hospitalization for heart failure. P values < 0.05 are shown in **bold**.

AU, Agatston unit; BNP, B-type natriuretic peptide; CABG, coronary artery bypass grafting; CT, computed tomography; ECV, extracellular volume fraction; eGFR, estimated glomerular filtration rate; LV, left ventricular; LVEF, left ventricular ejection fraction; NYHA, New York Heart Association; PCI, percutaneous coronary intervention; SAVR, surgical aortic valve replacement; STS-PROM, Society of Thoracic Surgeons Predicted Risk of Mortality; TAVR, transcatheter aortic valve replacement.

Table S2. Univariable Cox regression analysis for composite outcome in TAVR group.

	Univariable		
	HR	95% CI	p Value
Age, years	1.02	0.90–1.16	0.79
Male	1.59	0.60–4.24	0.37
Body mass index, kg/m ²	0.93	0.81–1.05	0.22
NYHA class III or IV	2.74	1.05–7.15	0.041
STS-PROM score, %	1.00	0.88–1.11	0.95
Atrial fibrillation	1.74	0.56–5.39	0.36
Coronary artery disease*	0.55	0.18–1.68	0.27
Implantable cardiac device	-	-	-
BNP, pg/ml	1.0006	0.9998–1.0012	0.12
LVEF, %	0.99	0.95–1.02	0.39
LV mass, g	1.00	0.99–1.01	0.36
E/e' ratio	1.00	0.96–1.03	0.85
Peak aortic-jet velocity, cm/s	1.01	0.99–1.02	0.21
Mean aortic valve gradient, mm Hg	1.04	0.99–1.08	0.052
Indexed aortic valve area, cm ² /m ²	0.43	0.005–39.73	0.71
Bicuspid aortic valve	2.51	0.33–19.06	0.43
Low-flow, low-gradient subtype	0.37	0.05–3.01	0.29
ECV, %	1.26	1.11–1.42	<0.001
Aortic valve calcium score, AU	1.0004	1.0000–1.0008	0.044

*Coronary artery disease defined as history of previous myocardial infarction, percutaneous coronary intervention, or coronary artery bypass grafting. P values < 0.05 are shown in **bold**. AU, Agatston unit; BNP, B-type natriuretic peptide; CI, confidence interval; ECV, extracellular volume fraction; HR, hazard ratio; LV, left ventricular; LVEF, left ventricular ejection fraction; NYHA, New York Heart Association; STS-PROM, Society of Thoracic Surgeons Predicted Risk of Mortality; TAVR, transcatheter aortic valve replacement.

Table S3. Univariable Cox regression analysis for composite outcome in SAVR group.

	Univariable		
	HR	95% CI	p Value
Age, years	1.05	0.89–1.26	0.58
Male	0.62	0.06–5.97	0.67
Body mass index, kg/m ²	0.71	0.44–1.06	0.098
NYHA class III or IV	4.36	0.61–31.08	0.16
STS-PROM score, %	1.27	1.05–1.62	0.014
Atrial fibrillation	20.16	2.06–197.79	0.005
Coronary artery disease*	1.86	0.26–13.3	0.54
Implantable cardiac device	5.67	0.50–64.08	0.22
BNP, pg/ml	1.003	0.999–1.006	0.12
LVEF, %	1.01	0.94–1.13	0.86
LV mass, g	0.98	0.96–1.00	0.11
E/e' ratio	1.04	0.99–1.10	0.098
Peak aortic-jet velocity, cm/s	0.99	0.98–1.00	0.096
Mean aortic valve gradient, mm Hg	0.96	0.90–1.01	0.13
Indexed aortic valve area, cm ² /m ²	19.39	0.17–3003.84	0.21
Bicuspid aortic valve	0.88	0.09–8.51	0.91
Low-flow, low-gradient subtype	20.47	1.75–238.84	0.016
ECV, %	1.87	1.15–3.99	0.009
Aortic valve calcium score, AU	0.9993	0.9981–1.0002	0.13

*Coronary artery disease defined as history of previous myocardial infarction, percutaneous coronary intervention, or coronary artery bypass grafting. P values < 0.05 are shown in **bold**. AU, Agatston unit; BNP, B-type natriuretic peptide; CI, confidence interval; ECV, extracellular volume fraction; HR, hazard ratio; LV, left ventricular; LVEF, left ventricular ejection fraction; NYHA, New York Heart Association; SAVR, surgical aortic valve replacement; STS-PROM, Society of Thoracic Surgeons Predicted Risk of Mortality.